



## Numerical Simulations of Collimator Insertions using MAFIA

C.D.Bear<sup>1</sup>, R.M.Jones<sup>1,2</sup>

November 01, 2006

### Abstract

This report concerns the simulation technique for longitudinal and transverse wakes, including results for some of the proposed collimator designs tested in the SLAC end station A wake-field tests. The purpose of this exercise is to verify existing simulation results and to expand the work to include the latest proposals for collimator designs. Several collimator designs including single steps to tapered structures have been simulated and the results are presented. For each of the test pieces proposed there are calculations of the transverse and longitudinal wake functions and the corresponding kick or loss factor. The angular deflection as a function of beam off set has also been calculated for a stepped collimator insertion. The total transverse kick presented to the beam is decomposed into its constituent multi-pole components and the dipole component is compared with an analytical model. The dipole kick factor is shown to be well-predicted by the analytical model.

---

<sup>1</sup> Cockcroft Institute, Daresbury Laboratory, Warrington, UK

<sup>2</sup> Department of Physics and Astronomy, The University of Manchester,  
Oxford Road, Manchester, M13 9PL, United Kingdom

<b>Numerical Simulations of Collimator Insertions using MAFIA .....</b>	<b>1</b>
<b>Abstract .....</b>	<b>1</b>
<b>1 Introduction .....</b>	<b>3</b>
<b>1.1 Theory .....</b>	<b>3</b>
<b>1.2 ESA Wake-field Tests .....</b>	<b>4</b>
<b>2 MAFIA Simulations .....</b>	<b>4</b>
<b>2.1.1 Method.....</b>	<b>4</b>
<b>2.1.2 Setting up the model.....</b>	<b>5</b>
<b>2.1.3 Defining the geometry .....</b>	<b>5</b>
<b>2.1.4 Meshing .....</b>	<b>5</b>
<b>2.1.5 Initial/Boundary conditions.....</b>	<b>6</b>
<b>2.1.6 Defining the beam.....</b>	<b>6</b>
<b>2.1.7 Monitors and test particle.....</b>	<b>6</b>
<b>2.1.8 Post-processing .....</b>	<b>7</b>
<b>2.1.9 Difficulties/Limitations .....</b>	<b>7</b>
<b>3 Results .....</b>	<b>8</b>
<b>3.1 Longitudinal wake potentials .....</b>	<b>8</b>
<b>3.1.1 Results for Slots 1,2 and 6 for varying bunch lengths.....</b>	<b>8</b>
<b>3.1.2 Results for Slots 4 and 5 for varying bunch lengths.....</b>	<b>9</b>
<b>3.1.3 Loss factor calculations for all slots.....</b>	<b>11</b>
<b>3.2 Transverse wake potential.....</b>	<b>12</b>
<b>3.2.1 Results for Slot 4 for varying bunch lengths.....</b>	<b>12</b>
<b>3.2.2 Kick Factor Calculations for slot 4.....</b>	<b>13</b>
<b>3.2.3 Angular deflection of an off-axis beam .....</b>	<b>13</b>
<b>3.2.4 Comparison of Kick Factor with analytic formula .....</b>	<b>15</b>
<b>4 Conclusion.....</b>	<b>15</b>
<b>5 Acknowledgement .....</b>	<b>16</b>
<b>6 References .....</b>	<b>16</b>
<b>7 Appendix A .....</b>	<b>18</b>
<b>Appendix B.....</b>	<b>19</b>

## 1 Introduction

The removal of halo particles having large divergence relative to the designed path is advantageous to minimise damage and to reduce background levels in the detector. Such levels are maintained in the ILC by placing a series of collimators along the beam path prior to the collision. The presence of these collimators induces short-range transverse wake-fields that may perturb the beam motion and lead to both emittance dilution and amplification of position jitter at the interaction point (IP).

A beam travelling through a beam pipe of constant cross section will not excite any geometric wake-fields. Although in practise the tube will have finite conductivity and will excite a resistive wall wake-field. A collimator will add an impedance mismatch wherever it is placed and will cause reflections in the electric field which could perturb subsequent bunches. As a charged bunch passes close to a metal surface a current/charge is induced in the surface of the metal, and a resultant electric field is produced. This could affect the beam dynamics in two ways:

- The head of the bunch can induce an instability along the bunch from the wake-field excited by the bunch. This is referred to as a short-range effect.
- If the wake-field has not diminished sufficiently by the time the second bunch arrives it can disturb the progress of this bunch and subsequent bunches. This is a long-range effect.

These wake-fields have both longitudinal and transverse components. There are three factors which enhance the effects of wake-fields: the geometry, the material and the surface finish. In this work we focus of geometrical changes on the wake-fields. For example, a sharp change in the impedance of the geometry results in a larger reflection in the fields, providing a large wake-field and a correspondingly large kick to the beam.

### 1.1 Theory

We consider the e.m. field due to point-like or  $\delta$  function charges. To this end, consider a single point-like charge moving close to the speed of light. This ultra-relativistic charge is surrounded by a wedge of e.m. field almost entirely transverse to the direction of its motion. At exactly the velocity of light the angle of this so-called ‘light cone’ shrinks to zero and the field is entirely transverse to the motion of the charge [1]. If the point-like charge travels down an infinitely long perfectly conducting beam pipe of constant radius then no wake-field is developed as the field induced by the charge travels with the charge.. However, should the radius of the pipe change, the e.m. field is scattered at the transition between beam pipes and a wake-field is developed. The collimators presented in this work present a scattering transition as far as the beam is concerned and will result in significant wake-field being developed. In order to analyse the wake-field we consider a second charge trailing behind the exciting charge. This witness charge travels at the same velocity  $v$  and for convenience is assumed to be located at an identical transverse coordinate, and at a distance  $s$  from the first charge. The fields excited by the driving charge,  $E(x,y,z,t=z/v)$ , and  $B(x,y,z,t)$  are seen at a later time  $dt=s/v$  by the witness charge. The Lorentz force experienced by the charge is given by:

$$\vec{F}(x, y, z, t) = e.(\vec{E}(x, y, z, (z+s)/|\vec{v}|)) + \vec{v} \times \vec{B}(x, y, z, (z+s)/|\vec{v}|) \quad (1)$$

The integral of this force along the  $z$  axis yields the wake potential

$$\vec{W}_{\parallel}(x, y, z, t) = \frac{1}{q} \int_{-\infty}^{\infty} (\vec{E}_{\parallel}(x, y, z, (z+s)/|\vec{v}|) + \vec{v} \times \vec{B}(x, y, z, (z+s)/|\vec{v}|)) dz \quad (2)$$

The longitudinal component of the wake-potential describes the energy loss of the test particles divided its charge and by the wake-field driving charge  $q$ . The transverse

component of the wake-potential is the change in the transverse test particle impulse divided by  $q$ . The transverse wake-potential is not uniquely defined, but it is conveniently presented in the form [1]:

$$\bar{W}_{\perp}(x, y, z, t) = \frac{1}{q\xi} \int_{-\infty}^{\infty} \left( \bar{E}(x, y, z, (z+s)/|\bar{v}|) + \bar{v} \times \bar{B}(x, y, z, (z+s)/|\bar{v}|) \right) dz \quad (3)$$

Where  $\xi$  is the transverse displacement of the charge.

In practise the bunch profile is not point-like but has a Gaussian distribution. To obtain the wake-field of a bunch with a Gaussian profile the wake-field of a point-like source is convolved with the Gaussian profile of the bunch shape.

Finally we note that the two components of the wake-field influence the charge in different ways. A charge distribution subjected to a longitudinal component of the wake-field results in an energy spread along the charge. This will result in an inefficient transfer of energy to the charge. On the other hand, the transverse wake-field can readily lead to a Beam Break Up (BBU) instability in the worst case, and at the very least can dilute the emittance of the accelerated beam. It is important to be able to accurately calculate these wake-fields in order that their impact on the beam be properly assessed.

## 1.2 ESA Wake-field Tests

A proposal was submitted to install a wake-field apparatus to the SLAC End Station A (ESA) beam line [2] in order to carry out wake-field tests using the collimator designs proposed in appendix A. The collimator designs vary in order to understand the effect of the taper gap size (first round, slot 2), resistive wall wakes (first round, slot 3), single stepped structures (first round, slot 4 and second round, slot 1 and 2), taper angles (second round slots # 2, 3 and 4).

This report concerns the results slots 1, 2, 4, 5 and 6.

## 2 MAFIA Simulations

MAFIA [3] has built in function that allows the user to measure the integrated wake-field as a function of  $s$ , the distance behind the source particle. This enables the user to record the long range wake-field behind a simulated bunch that can then be transformed into the frequency domain to produce a broad-band impedance of the structure.

To carry out the wake-field calculations, Maxwell's equations are transformed into a set of discrete matrix equations using the finite integration technique. This set of equations can then be solved using the time domain solver (T-3). A particle beam travelling through the structure is simulated and a witness particle is used to calculate the wake potential.

This technique has already been applied to some of the collimator shapes tested at SLAC [4]. The calculations and computer models generated at SLAC were used as a starting point for setting up the models, since these were successfully benchmarked with previous experimental data.

### 2.1.1 Method

There are two techniques to calculating the wake integration, the direct and the indirect method;

- The direct integration technique computes the time integral over the EM forces from the fields in the range. This method is limited by numerical noise.
- The indirect method, calculates the EM field at the location of the walls of the surrounding cylinder to calculate the wake integral. This method has been extended to cases in which irises and other transitions have a smaller radius than the surrounding beam pipes [5]. However, the present version of MAFIA we are using does not take

advantage of the latter development. For the collimator simulations the indirect method has been applied.

### 2.1.2 Setting up the model

For the case of the collimator insertions, the simulations are considerably more efficient if we take advantage of the inherent symmetry planes of the system. There are two planes of symmetry, in both the x and the y direction. The symmetry in the y-axis can only be used for the longitudinal wake-field calculations. Once the beam is off-set in the y-direction, the model is no longer symmetrical in the y-plane, hence only the x-axis symmetry plane can be utilised for the transverse wake-field calculation. Fig. 1 shows a 3D CAD model of the collimator insertions, illustrating the symmetry planes in the X and Y plane. By selecting symmetry planes the size of the calculated region is reduced and hence, the simulations will be smaller and solve more rapidly.

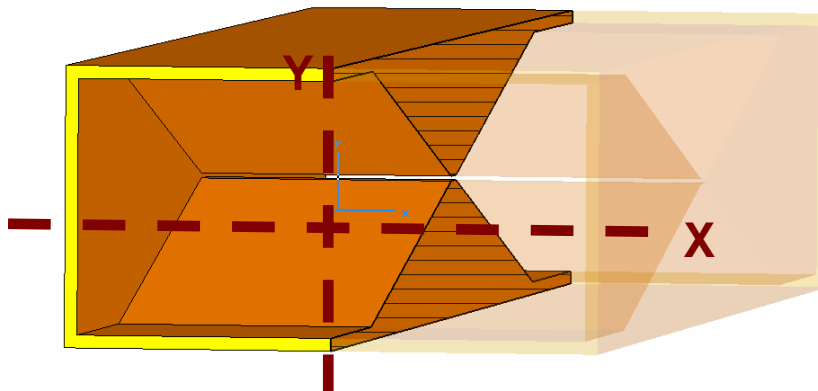


Figure 1 Collimator Schematic with symmetry planes

### 2.1.3 Defining the geometry

For reproducibility and repeatability, the geometry is set up using ‘self-defined’ variables. In this manner the models are quickly altered for the different structure dimensions, with the same simulation conditions (described below) initiated. An example of the command file can be seen in appendix B.

The inside volume of the collimator is defined as a brick, which has is three times the length of the insertions, to allow enough space either side of the geometry, in order for the fields to decay easily. The collimator insertions are defined as a surface that is extruded the width of the beam pipe.

### 2.1.4 Meshing

The mesh is the critical section, which controls the resolution and the accuracy of the results. In order to obtain an adequate resolution, at least 10 mesh cells per bunch length are required. Due to the length of the bunch required to imitate ILC conditions, long structures are excluded as the mesh requirements are too large for the PC based system. The ILC bunch length is 300  $\mu\text{m}$ , therefore it is required to have mesh cells 30  $\mu\text{m}$  in cell length. The larger the mesh the larger the amount of memory required, hence the difficulties solving for larger structures with short bunch lengths.

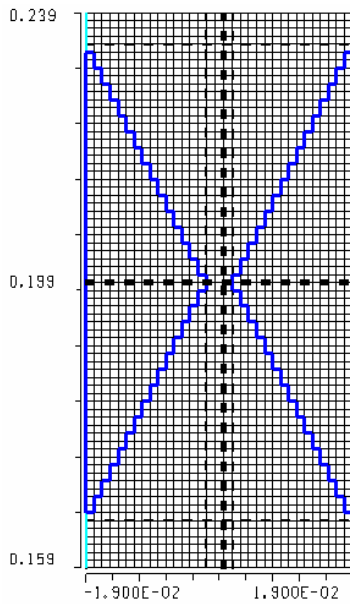


Figure 2 Stair cased geometry

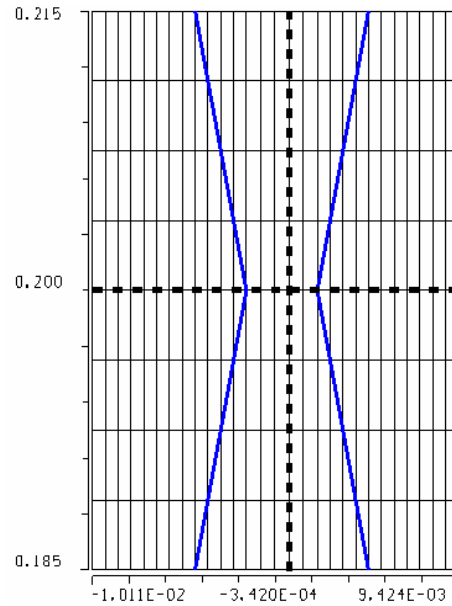


Figure 3 Geometry using diagonal cells

MAFIA is based on a finite difference algorithm and it uses a quadrilateral mesh to model the geometry. This makes it difficult to adequately model tapered structures without recourse to a large mesh density. With a course mesh, steps in the tapered geometry become very clear, see Fig. 2. The stepped structure does not, of course, map out the exact geometry and introduces numerical noise into the calculation. MAFIA is capable of meshing half cells along the diagonal, allowing tapered structures to be accurately modelled (Fig. 3). However due to the angle of the tapers, the aspect ratio for the proposed shapes would be such that the numerical uncertainty in having long thin mesh cells would add no benefit in using the diagonal cells.

### 2.1.5 Initial/Boundary conditions

The model is set-up such that the main volume is a vacuum and is bounded by perfectly conducting material, and the material for the collimator insertions is also chosen to be perfectly conducting purely for simplicity. For this reason only the geometric wake-field is calculated. The entrance and exits to the beam pipes are perfectly matched ports in order to completely absorb the outgoing fields and to avoid any reflections at the port that would effect the wake-field calculations.

### 2.1.6 Defining the beam

For the longitudinal wake-field the beam travels through the centre of the beam pipe, and for the transverse calculations there is a defined off-set. The beam has a Gaussian profile and is chosen to have a charge of one Coulomb for the calculation. The real charge is assigned during the post processing. Due to the point charge travelling along a symmetry plane, calculations have to take into account possible duplication of the charge once scaled up. The bunch length is defined as Sigma, and the simulation runs long enough for the bunch to pass through the collimator and for its fields to decay.

### 2.1.7 Monitors and test particle

Monitors are set-up to store the wake potential throughout the model. For the calculation of the loss factors and kick factors a test particle is chosen to be an arbitrary distance behind the particle and the resultant force on the particles determines this loss.

### **2.1.8 Post-processing**

The monitors set automatically store the wake-potential in units of Volts per pico Coulomb (V/pC). In order to calculate the corresponding loss factor or kick factor an integration of this wake-potential profile with the bunch is required. This is carried out during post-processing.

### **2.1.9 Difficulties/Limitations**

Difficulties simulating the tapered collimator shapes arose due to mesh limitations. For accuracy it is recommended to use a minimum of 10 mesh cells per bunch length. Due to memory constraints this made it possible to simulate the collimators quite easily up to 1mm bunch lengths. For the 0.5mm bunch lengths a cruder mesh was adopted, typically about 5 to 6 mesh cells per bunch length.

The step collimators were successfully simulated at the short bunch lengths, however, these proved to be on the limit of capability.

### 3 Results

In this section the results from the MAFIA simulations are presented. The results have been grouped into the tapered collimators and the step collimators.

#### 3.1 Longitudinal wake potentials

##### 3.1.1 Results for Slots 1,2 and 6 for varying bunch lengths

The following graphs are plots of the longitudinal wake-potential for slots 1,2 and 6 for bunch lengths of 5mm, 1mm and 500 microns. Fig. 4 highlights the longitudinal wake-potential witnessed by a subsequent particle as a function of distance behind. As expected for two similar geometries (slots 1 and 2) as the gap is slightly reduced and the maximum field witnessed was slightly higher. Since the mesh of these two structures was almost identical, a realistic comparison is obtained. A comparison of slots 2 and 6 suggest that as the taper angle is reduced, the effective impedance is decreased for the same gap size. Comparing slots 2 and 6, it is suggested that two collimators of equal gap size should show a decrease in loss factor as the taper angles decrease. This can be explained as the taper angle decreases the impedance rate of change decreases lowering the impedance.

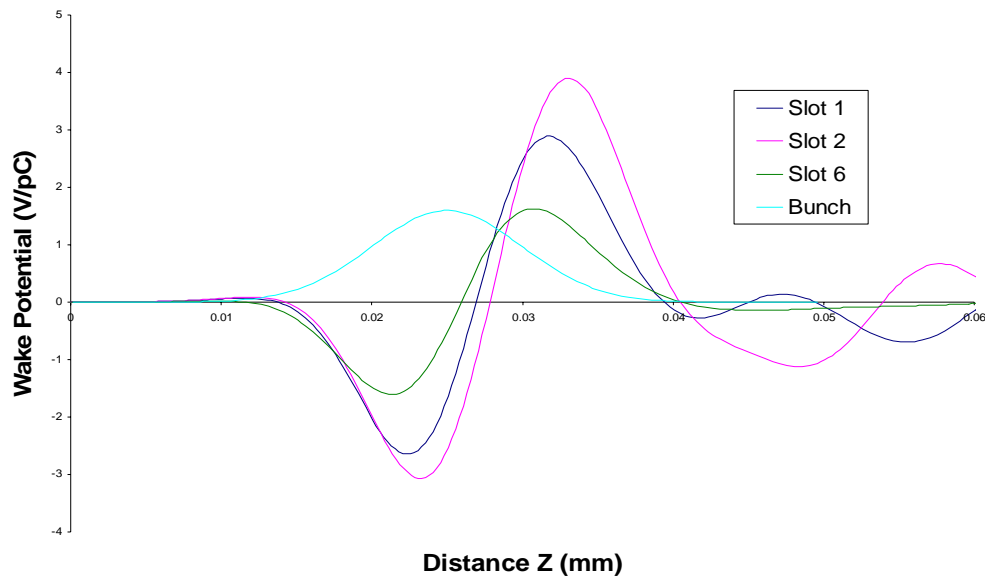
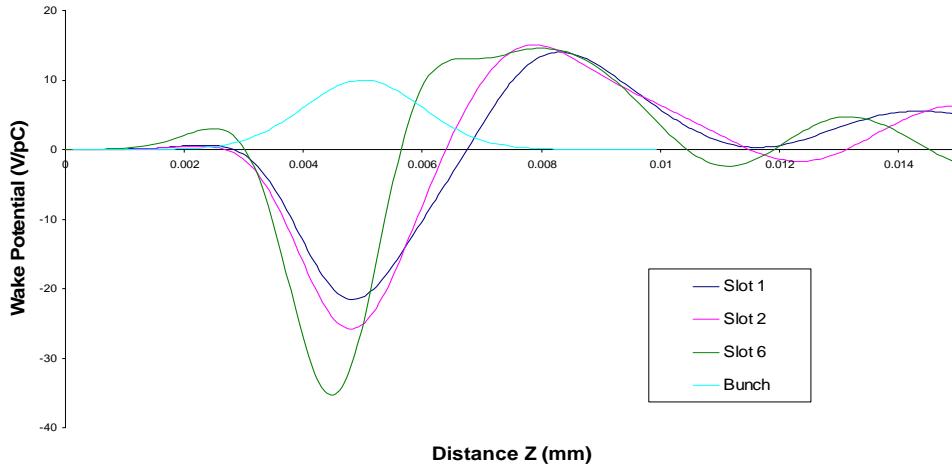


Figure 4 Longitudinal Wake - 5mm Bunch length

At shorter bunch lengths the mesh requirement is such that sacrifices have to be made in the mesh density in order to solve for the collimators. Comparing slots 1 and 2, there is a direct comparison with the results for the 5mm bunch length. Here, it also shows an increase in wake-potential as you close the gap from 4mm to 2mm. For the case of the longer collimator (slot 6), you would also expect that the wake-potential is reduced due to the shallower taper angle as with the 5mm bunch lengths. However, due to the restraints on mesh (effectively addressable memory), the resolution of the mesh had to be reduced significantly in order for the calculation to compute. Such a decline in mesh quality has lead to incorrect results. For this reason it is not a true comparison of collimator shape with respect to bunch length. For this simulation, 5 Gb of RAM were required, windows based systems only allow a maximum of 1.4 Gb of memory to be addressed by each application, permitting a maximum of 2 mesh cells per bunch length which is insufficient to provide the necessary resolution.



**Figure 5 Longitudinal Wake - 1mm Bunch length**

Similar comparisons can be made for the 500 micron bunch lengths, suggesting that a higher resolution is required for the longer tapered structures. Figs. 5 and 6 also show similar trend as for the wake-potential results of slot 6.

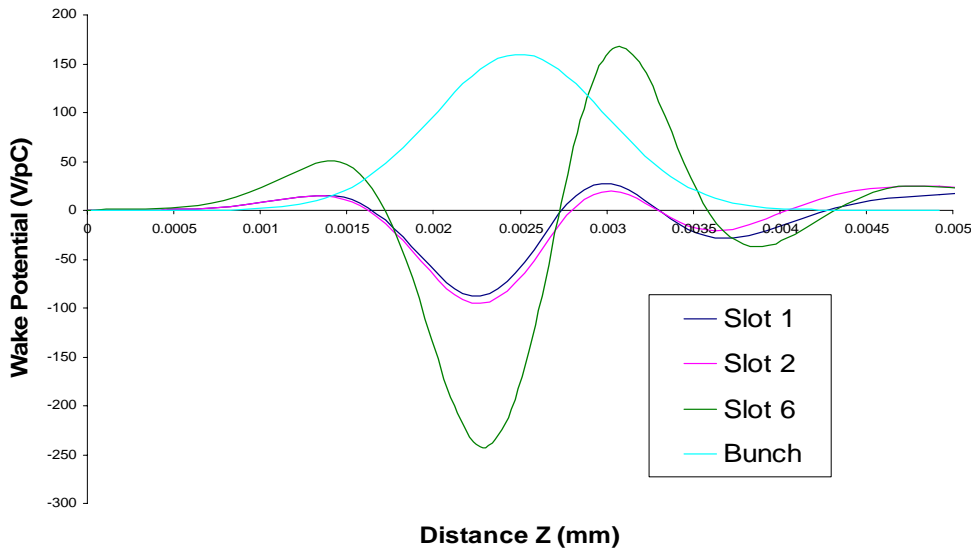


**Figure 6 Longitudinal Wake - 500 μm Bunch length**

### 3.1.2 Results for Slots 4 and 5 for varying bunch lengths

The following graphs are plots of the longitudinal wake-potential for slots 4 and 5 for bunch lengths of 5mm, 1mm and 500μm. Due to the shorter length of the step collimators, an adequate mesh resolution was achieved, albeit slightly reduced for the 500 μm bunch lengths (6 mesh cells per bunch length).

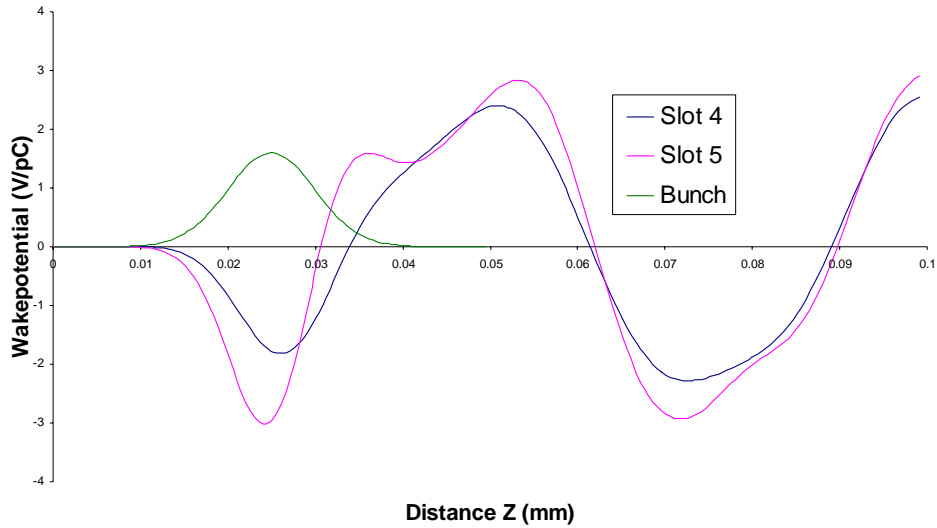


**Figure 7 Step Longitudinal Wake-potential 5mm**

As expected, as the bunch length is reduced the wake-potential rises for identical structures.

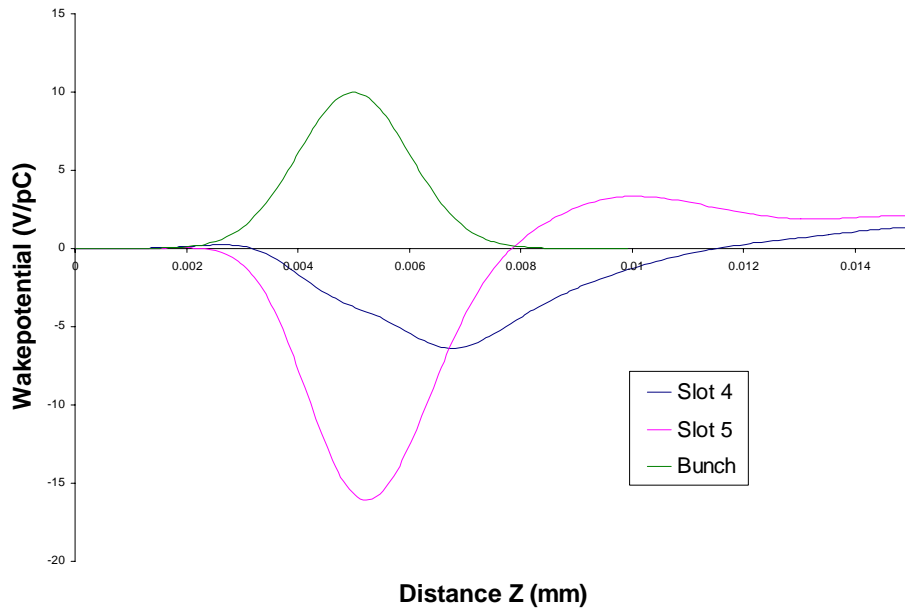


**Figure 8 Step Longitudinal Wake-potential 1mm**

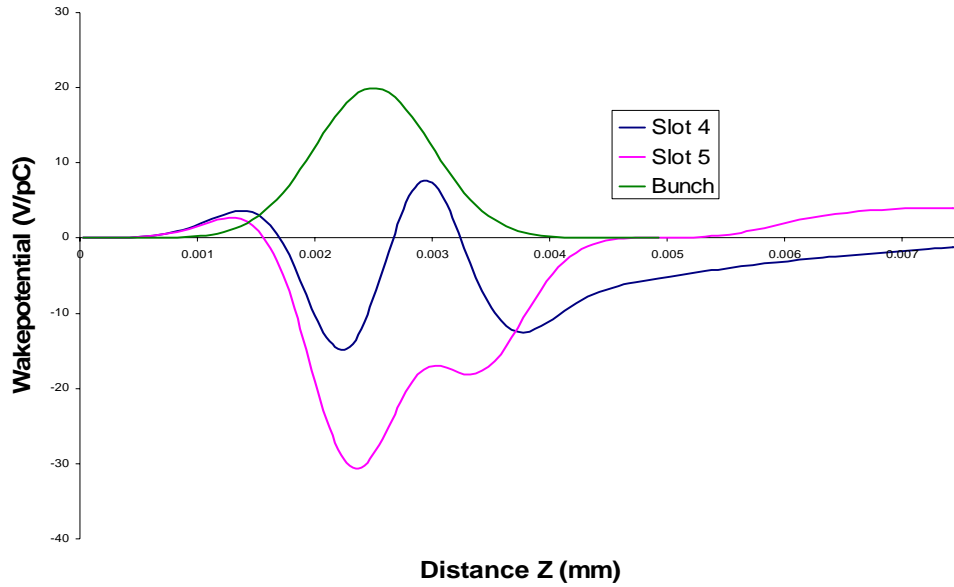


Figure 9 Step Longitudinal Wake-potential 500µm

**3.1.3 Loss factor calculations for all slots.**

The loss factor is calculated by integrating the wake-potential along the bunch profile. There is an in-built function in MAFIA for this purpose. A summary of the loss factors are contained in Table 1 below.

Table 1 Loss Factor Results Summary

	5mm Bunch	1mm Bunch	0.5mm Bunch
Slot 1	-0.6	14.01	34.75
Slot 2	0.89	15.67	42.16
Slot 3			
Slot 4	1.185	3.379	4.76
Slot 5	1.7	11.254	20.57
Slot 6	0.23	15.44	72.42

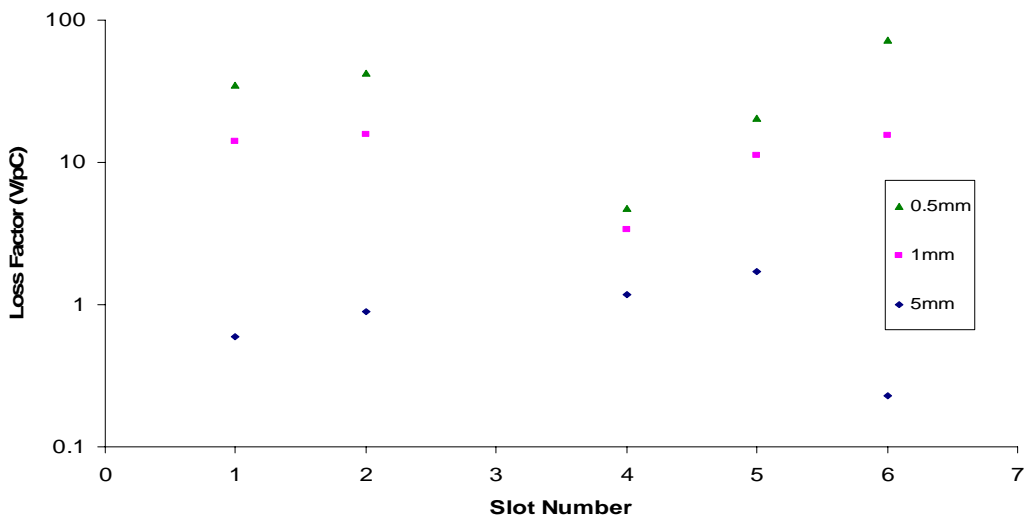


Figure 10 Longitudinal Loss Factors

Fig. 10 displays the longitudinal loss factors on a logarithmic scale as a function of bunch length for each collimator slot simulated. The results show a considerable rise in the loss factor for the longer tapered structure (slot 6), compared with that of the shorter taper (slot 2) and the step collimator (slot 5). All three of these have the same gap dimension of 2.8 mm, with the lowest loss factor arising from the step profile. As discussed previously, this is due to the decrease in Mesh resolution achievable for the shorter bunch length. Therefore, for realistic simulations only the longer 5mm bunch lengths should be considered.

Comparing the loss factors for the 5mm bunch length, an order of magnitude increase is observed from the step collimators compared with the tapered structures, with the lowest loss factor arising from the shallower tapered collimator (slot 6) as predicted. However, the shorter bunch lengths produce incorrect results as it is not possible to produce an X-Y-Z mesh that models the actual geometry with sufficient accuracy on PC based machines.

### 3.2 Transverse wake potential

Calculations of the transverse kick factor have been calculated using MAFIA. Due to the difficulties experienced achieving sufficient mesh for the larger structures only Slot 4 (step) has been assessed for transverse wake-fields. This has allowed bunch structure up to 500  $\mu\text{m}$  to be simulated.

In order to calculate the transverse wake potential, the trailing beam travels collinear to the driving beam path at a specified offset with respect to the electrical centre of the collimator. . The off-set lies along the y-axis, and the measurement is taken as a function of distance behind the particle on the beam axis.

#### 3.2.1 Results for Slot 4 for varying bunch lengths

Results for slot 4 are displayed in Fig. 11. As the beam is displaced further off axis, the wake-potential measured along the centre of the device reduces.

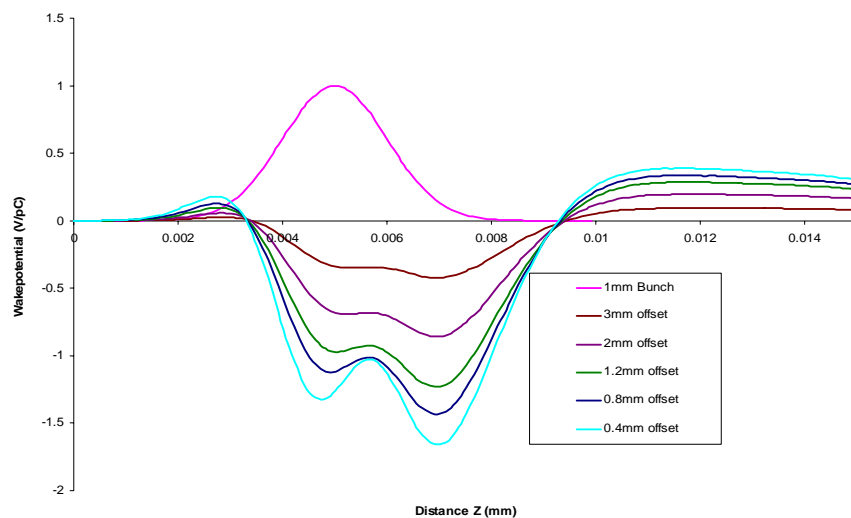


**Figure 11 Transverse wake-potential 1mm bunch length**

Figure 12 displays the wake-potential calculated from an analysis of the step collimator with a 500 micron bunch length.

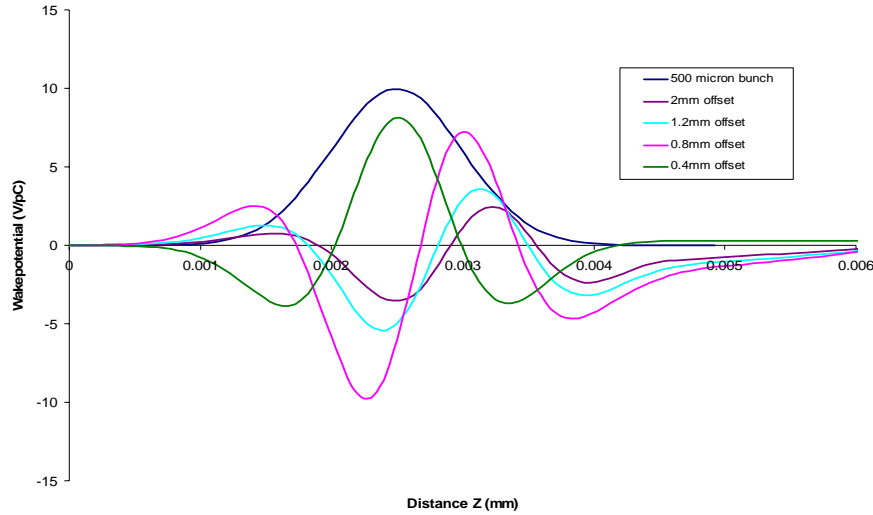


Figure 12 Transverse wake-potential 500 micron bunch

### 3.2.2 Kick Factor Calculations for slot 4

The kick factor is calculated by integrating the wake potential along the bunch profile and dividing by the beam off-set. The results for the slot 4, for both 1mm and 500 $\mu$ m as a function of beam offset are displayed in Table 2. This data can then be used to determine the deflection the beam would receive.

Table 2 Kick Factors Results Summary

Bunch length	1mm	1mm	1mm	1mm	1mm	1mm	1mm	1mm	1mm	1mm	1mm
Off-set (mm)	-3	-2	-1.2	-0.8	-0.4	0	0.4	0.8	1.2	2	3
Loss (V/pC)	0.0827	0.165	0.223	0.233	0.164	0	0.164	0.233	0.223	0.165	0.0827
Kick (V/pC/mm)	-0.0276	-0.083	-0.186	-0.2913	-0.41	0	0.41	0.2913	0.1858	0.0825	0.0276
Bunch length		0.5mm	0.5mm	0.5mm	0.5mm	0.5mm	0.5mm	0.5mm	0.5mm	0.5mm	
Off-set (mm)		-2	-1.2	-0.8	-0.4	0	0.4	0.8	1.2	2	
Loss (V/pC)		0.364	0.777	1.298	2.948	0	2.948	1.298	0.777	0.364	
Kick (V/pC/mm)		-5.495	-1.544	-0.6163	-0.1357	0	0.1357	0.6163	1.5444	5.4945	

### 3.2.3 Angular deflection of an off-axis beam

Once the kick factor has been calculated for a given offset, it is then possible to calculate the deflection obtained from the resultant wake potential observed. The ratio of the transverse offset to the incremental distance travelled is the same as the ratio of transverse to longitudinal beam energy;

$$\frac{\delta y}{\delta z} = y' = \sum \frac{Ne^2 K_n y^n}{\gamma mc^2} \quad (4)$$

Where  $N$ , denotes the number of particles in the bunch ( $10^{10}$  particles for ILC/ESA bunch),  $\gamma$  is the relativistic factor (500 for ESA,  $\sim 20000$  for ILC),  $K$  is the kick factor and  $n$  represents the  $n^{th}$  multi-pole. Hence  $K^n$  is the  $n^{th}$  multi-pole component of the kick factor. For the dipole mode this reduces to:

$$y' = \frac{Ne^2 Ky}{\gamma mc^2} \quad (5)$$

The classical radius of the electron is given by;

$$r_e = \frac{1}{4\pi\epsilon_0} \frac{e^2}{mc^2} \quad (6)$$

Substituting for (6) removes the  $e^2/mc^2$  term, simplifying Eq. 5 to;

$$y' = \frac{NKy}{\gamma} r_e (4\pi\epsilon_0) \quad (7)$$

For a general multi-pole, the equation becomes;

$$y'_n = \frac{NK_n y^n}{\gamma} r_e (4\pi\epsilon_0) \quad (8)$$

The calculations performed in this report have been solved in the time domain. The transverse kick that results from these calculations is effectively the sum of all multi-poles. In order to assess the individual contributions of dipole kick factors and higher order multi-pole we the overall deflection of the beam is decomposed into a sum of multi-poles:

$$y' = \sum_{\infty} y'_n = \sum_{\infty} \frac{NK_n y^n}{\gamma} r_e (4\pi\epsilon_0) \quad (9)$$

$$\Rightarrow y' = \sum_{\infty} y'_n = \frac{Nr_e (4\pi\epsilon_0)}{\gamma} (K_1 y + K_2 y^2 + K_3 y^3 + \dots) \quad (10)$$

Here,  $K_1$ ,  $K_2$  and  $K_3$  are the dipole, quadrupole and sextupole kick factor components of the multi-poles respectively. In order to determine the deflection as a function of beam offset, simulations have been undertaken. The deflections have been calculated for a bunch of length 500  $\mu\text{m}$  traversing slot 4. Once the data has been analysed from the ESA beam test we anticipate making detailed comparisons with our simulations

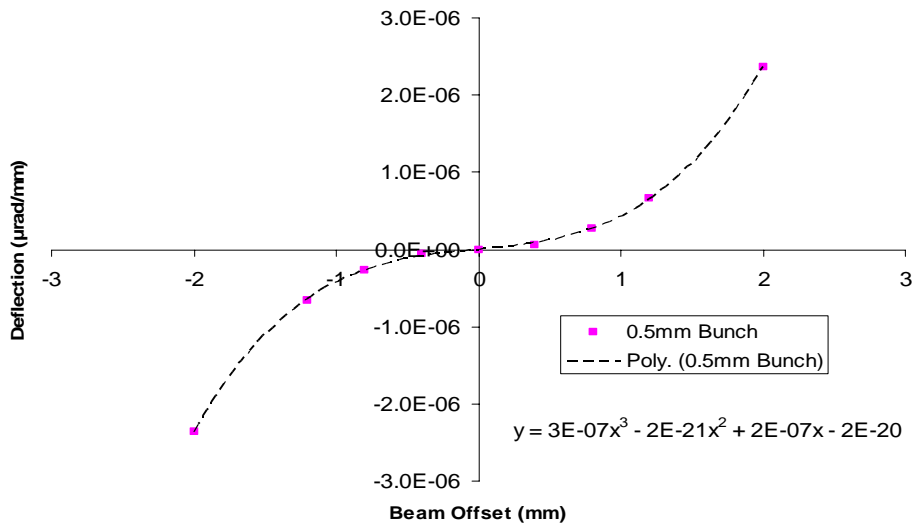


**Figure 13 Normalised deflection of the bunch as a function of offset**

In agreement with theory, as the beam is displaced closer to the collimator the deflection generated from the short range wake-field increases asymptotically to the separation distance of the collimators. At an offset of 2mm the calculations suggest a deflection of 74  $\mu\text{rad}$ . This should be confirmed with experimental data, once the data analysis from the ESA wake-field tests have concluded.

### 3.2.4 Comparison of Kick Factor with analytic formula

Analytic calculations have been carried out to determine the kick factor due to the dipole component. To compare with our numerical simulations we make an expansion of the total kick in terms of multi-poles. This entails making a polynomial fit to the numerical data in powers of  $x^n$  (where  $n \geq 1$ ).

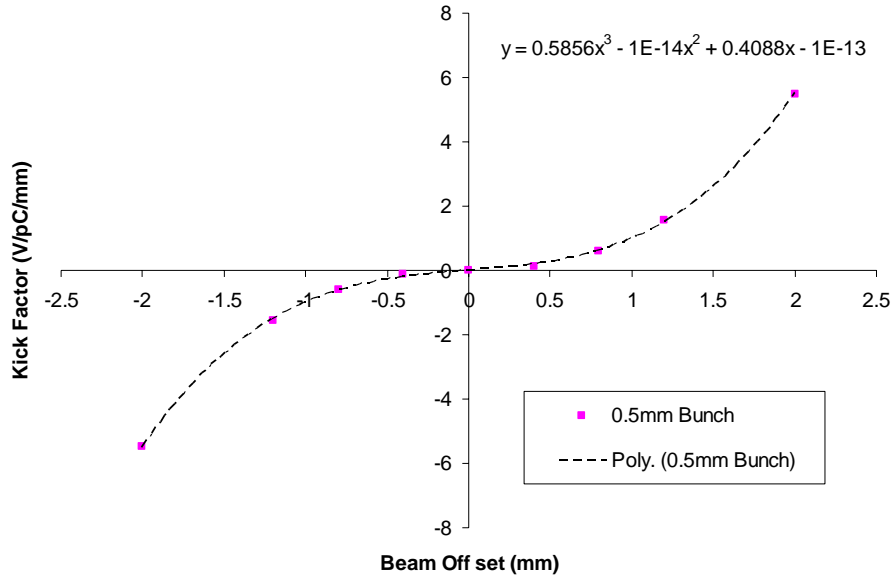


Figure 14 Kick Factor as a function of off-set

A 3<sup>rd</sup> order polynomial fit of the curve in Fig. 14 has been carried out and can be compared with equation 10. An excellent fit has been achieved, demonstrating that terms no higher than sextupoles are needed. The polynomial fit is expressed in Eq. 11.

$$y = 0.5856x^3 + 0.4088x \quad (11)$$

Comparing Eqs.s 10 and 11, the dipole kick factor is 0.408 V/pC/mm. Furthermore, as the width of collimator 4 is much larger than the gap width we are able to use an analytical formula to approximate the dipole kick factor [6]:

$$K = \frac{1}{4\pi\epsilon_0} \frac{1}{b^2} \quad (12)$$

Where  $b$  ( $= 4$  mm) is the half-gap width. This analytical formula applies for a large aspect ratio of collimator width to gap width. For the parameters of the simulation, from Eq, 12 we obtain a kick factor of 0.562 V/pC/mm. This compares reasonably well with the dipole component of the multi-pole expansion which is 0.41 V/pC/mm. Thus, to within ~30% the analytic result is able to predict the dipole term. The sextupole kick factor is 0.5856 V/pC/mm<sup>3</sup>. For small offsets ( $\leq 0.75$ mm) the dipole kick is clearly the dominant term. However, for larger offsets the sextupole kick makes an important contribution.

## 4 Conclusion

A substantial fraction of the collimator slots have been studied. In the simulations presented only those with relatively long bunch-lengths have produced physical results for the collimators under consideration for the ILC. In particular, we have found that bunch lengths shorter than 5 mm required mesh densities that are larger than the available memory that can

be addressed on a standard PC. However, simulations with a 5 mm bunch length compare well with analytical models for the dipole component of the kick imparted to the beam. The corresponding angular deflection for slot 4 of the suite of collimators under test, is predicted to be 74  $\mu$ rad for a beam initially offset by 2 mm. Once the ESA data has been fully analysed it will be interesting to compare this predicted offset with the experimentally determined values.

One means of reducing the mesh requirements is to simulate an artificial structure, namely a cylindrical collimator and then make use a suitable transformation constant to relate the wake-field simulated in the cylindrical structure to the actual rectangular collimator. This allows symmetry planes to be inserted into the geometry and enables a considerable saving to be made in the required mesh density. However, this is only successful for on-axis beams as off-axis beam is equivalent to a ring of charge and it is not clear how to relate the results for the transverse wake-field to that expected to be excited in the rectangular geometry.

Finally we note that there are alternative and indeed complementary simulations that can be undertaken in order to simulate the wake-field that is excited by ILC bunches (where  $\sigma_z = 300 \mu\text{m}$ ). In order to make these simulations one can either use a computer code that uses a 'moving mesh' [7] or increase the mesh density. In order to pursue the latter method it is required to be able to address additional memory. GdfidL[8, 9], for example, is a natural choice for this as it is readily able to address more memory on a linux based machine. To this end, simulations are in progress at the Cockcroft Institute using GdfidL and on the moving mesh technique at DESY.

## 5 Acknowledgement

The assistance of Cho Kuen-Ng from Stanford Linear Accelerator Centre, California, in setting up the models and the further understanding of the MAFIA time domain solver is greatly appreciated.

This work is supported by the Commission of the European Communities under the 6th Framework Programme, "Structuring the European Research Area", contract number RIDS-011899.

## 6 References

- [1] B.W. Zotter and S.A. Kheifets, *Impedances and Wakes in High-Energy Particle Accelerators* (World Scientific, London), 2000.
- [2] N.K. Watson *et al.*, Direct Measurement of Geometric and Resistive Wakefields in Tapered Collimators for the International Linear Collider, Proceedings of the 10<sup>th</sup> European Particle Accelerator Conference, (EPAC06), MOPLS066, Edinburgh, 2006. Also SLAC-PUB-12029.
- [3] [www.cst.de](http://www.cst.de).
- [4] C.Ng *et al.*, Numerical Calculations of Short-Range Wake-fields of Collimators, Proceedings of the 19<sup>th</sup> IEEE Particle Accelerator Conference (PAC01), Chicago, p. 1853, 2001. Also SLAC-PUB-9078.
- [5] I.A. Zagorodnov, [Indirect methods for wake potential integration](#), Phys. Rev. ST Accel. Beams, 9, 102002, 2006.
- [6] G. Stupakov, High frequency impedance of small angle collimators, Presented at IEEE Particle Accelerator Conference (PAC2001), Chicago, 2001. Also, SLAC-PUB 9375.
- [7] K.L.F Bane, I.A Zagorodnov, Wakefield Calculations for 3D Collimators, Proceedings of the 10<sup>th</sup> European Particle Accelerator Conference (EPAC06), THCPH072, Edinburgh, 2006. Also SLAC-PUB-11938.

[8] W.Bruns, The Gdfidl Electromagnetic Field Simulator, CERN, [http://cllic-meeting.web.cern.ch/cllic-meeting/2005/10\\_07wb.pdf](http://cllic-meeting.web.cern.ch/cllic-meeting/2005/10_07wb.pdf), 2004.

[9] <http://www.gdfidl.de/>.

## 7 Appendix A

Collimator insertions tested at SLAC ESA in April/July 2006

Slot	Side view	Beam view	
1			$\alpha=335\text{mrad}$ $r=1.9\text{mm}$
2			$\alpha=335\text{mrad}$ $r=1.4\text{mm}$
3			$\alpha=335\text{mrad}$ $r=1.4\text{mm}$
4			$\alpha=\pi/2\text{rad}$ $r=3.8\text{mm}$

Slot	Side view	Beam view	
1			$\alpha=\pi/2\text{rad}$ $r=1.4\text{mm}$
2			$\alpha=168\text{mrad}$ $r=1.4\text{mm}$
3			$\alpha_1=\pi/2\text{ rad}$ $\alpha_2=168\text{mrad}$ $r_1=3.8\text{mm}$ $r_2=1.4\text{mm}$
4			$\alpha_1=298\text{mrad}$ $\alpha_2=168\text{mrad}$ $r_1=3.8\text{mm}$ $r_2=1.4\text{mm}$

## Appendix B

**\$ Command file comments have a dollar sign at the beginning of the line.**

**\$ First stage to define the variables that are to be used in the simulation.**

```
define 'xlen' = "0.038"
```

```
define 'ylen' = "0.038"
```

```
...
```

```
...
```

```
define 'z3' = "zlen/2+colth"
```

```
define 'z4' = "zlen"
```

**\$ Definition of the manual mesh and cell spacing to be used for the calculations**

```
#om
```

```
#general
```

```
geometry=xyz
```

```
lineaccuracy=2e-014
```

```
areaaccuracy=2e-014
```

```
volumeaccuracy=2e-014
```

```
scale=1
```

```
#mesh
```

```
automesh=no
```

```
ratiolimit=10.0
```

```
#model
```

```
usecad=yes
```

**\$ Here the mesh is generated, ensuring sufficient mesh between the beam axis and the collimator, as well as an equidistant mesh along the beam direction, for the final calculations a resolution of 10 mesh cells per bunch length in all planes was chosen.**

```
#mesh
```

```
xmesh "0.0" s "xm" "xlen/2"
```

```
ymesh "y0" s "ymcol" "y1" s "ymgap" "y2" s "ymcol" "y3"
```

```
zmesh "z0" s "(z4-z0)/ddz" "z4" execute
```

**\$ Vac Defines the volume space for the calculations.**

```
#om
```

```
#brick
```

```
action=replace
```

```
material="1"
```

```
name=vac
```

```
xlow ="0.0"          xhigh="xlen/2"
```

```
ylow ="-ylen/2"     yhigh="ylen/2"
```

```
zlow ="0.0"          zhigh="zlen"
```

```
quality="1.0" transform=unity filltype=solid fillmode=diagonal execute
```

**\$ Defines the tapers,**

```
#om
```

```
#cylinder
```

```
action=replace
```

```
material="2"
```

```
name=coll_1
```

```
orientation=x
```

```
range="0.0","xlen/2"
```

```

point="ylen/2","zlen/2-colth" line
point="ylen/2","zlen/2+colth" line
point="ylen/2-colhe","zlen/2" line
point="ylen/2","zlen/2-colth"
fillmode=diagonal filltype=solid quality="1.0" transform=unity execute

```

```

#om
#cylinder
action=replace
material="2"
name=coll_2
orientation=x
range="0.0","xlen/2"
point="-ylen/2","zlen/2-colth" line
point="-ylen/2","zlen/2+colth" line
point="-ylen/2+colhe","zlen/2" line
point="-ylen/2","zlen/2-colth"
fillmode=diagonal filltype=solid quality="1.0" transform=unity execute

```

```

#om
#model (Import the shapes [order important] and mesh)
reset
action=add
name=vac execute
name=coll_1 execute
name=coll_2 execute
action=remodel execute

```

### **\$ T3 Solve using beam**

```

#ot3
#material
mat=2 type=electric (Material defined as Perfect electrical conductor)
mat=1 epsilon=1 mu=1 (Material defined as Vacuum)
#boundary
xboundary=magnetic,electric (Symmetry plane in xmin used)
yboundary=electric,electric
zboundary=waveguide,waveguide

```

```

#beam
beamdirection=zaxis (beam position and direction)
xpos=0.0
ypos=0.0
beta=1 (Assumed to be travelling at c)
bunch=gaussian (bunch is assumed gaussian)
sigma=5e-3 (5mm bunch length)
isigma=5
charge=1e-12 (1 picocoulomb bunch charge)

```

```

#time ?
usmt ?

```

#monitor **(Monitors to store the wake-potentials)**

```
type=wake
symbol=wakeint
component=z
xpoint="0.0"
ypoint="0.0"
slow=0 shigh=50e-3 isstep=1
execute
```

```
#monitor
type=wake
symbol=wakey
component=y
xpoint="0.0"
ypoint="0.0"
slow=0 shigh=50e-3 isstep=1
execute
```

```
#monitor
type=wake
symbol=wakex
component=x
xpoint="0.0"
ypoint="0.0"
slow=0 shigh=50e-3 isstep=1
execute
```

```
#time
nend @integer00 ?
```

```
#control
mapstep=1 dumsave=no usebuffer=yes
execute
```

```
#op
#fft (Calculates the fast fourier transform of the wake-potential)
act=fft sym=wakeint execute
act=pol sym=wakeinre_f7 execute
```